

Navigating challenges in the application of superresolution microscopy

Talley J. Lambert and Jennifer C. Waters

Department of Cell Biology, Harvard Medical School, Boston, MA 02115

In 2014, the Nobel Prize in Chemistry was awarded to three scientists who have made groundbreaking contributions to the field of superresolution (SR) microscopy (SRM). The first commercial SR microscope came to market a decade earlier, and many other commercial options have followed. As commercialization has lowered the barrier to using SRM and the awarding of the Nobel Prize has drawn attention to these methods, biologists have begun adopting SRM to address a wide range of questions in many types of specimens. There is no shortage of reviews on the fundamental principles of SRM and the remarkable achievements made with these methods. We approach SRM from another direction: we focus on the current practical limitations and compromises that must be made when designing an SRM experiment. We provide information and resources to help biologists navigate through common pitfalls in SRM specimen preparation and optimization of image acquisition as well as errors and artifacts that may compromise the reproducibility of SRM data.

Introduction

Biologists eager to exploit the promises of a fast-moving field are quickly adopting superresolution (SR) microscopy (SRM), primarily using commercial SR microscopes. SRM is a technique that can greatly reward the rigorous user but has the potential to punish the casual user. To achieve optimal and reproducible results, SRM requires careful planning of specimen preparation, rigorous attention to instrument optimization and image acquisition, and a thorough understanding of the practical limitations, sources of error, and artifacts.

Our perspective on SRM comes from running core facilities in which we offer advice and training on commercial SRM instruments to a large and diverse research community and from teaching SRM in courses within and outside of our home institution. Our discussions with biologists interested in using SRM often reveal misunderstandings of the challenges

Correspondence to Jennifer C. Waters: jennifer_waters@hms.harvard.edu

Abbreviations used: FOV, field of view; FRC, Fourier ring correlation; HILO, highly inclined and laminated optical sheet; ISM, image-scanning microscopy; PAINT, point accumulation for imaging of nanoscale topography; PSF, point spread function; SIM, structured illumination microscopy; SMLM, single-molecule localization microscopy; SNR, signal to noise ratio; SR, superresolution; SRM, SR microscopy; STED, stimulated emission depletion; TIRF, total internal reflection fluorescence.



we discuss in this review. Surveying the rapidly growing body of publications that use SRM to address biological questions raises multiple causes for concern. There is dramatic variability in the quality of published SRM images, even among publications with images of the same sample with the same reported resolution, so we begin our discussion with image acquisition and specimen preparation parameters that affect resolution and image quality. Some publications report theoretically impossible resolutions; we discuss the difficulties in estimating the resolution achieved in SRM images and review different methods that can be used. There are publications containing SRM images with avoidable artifacts, or that do not report critical controls or image corrections. We review sources of artifacts and errors that must be addressed to generate accurate and reproducible SRM data and methods of optimizing SRM using standards and quantitative metrics. The trade-offs made to achieve multiwavelength, 3D, and live-cell SRM are not always clear in publications; we discuss compromises inherent to these methods. Some published studies include SRM figures with image scale bars that reveal that diffraction-limited microscopy would have been sufficient. We conclude our review with suggestions for when diffraction-limited microscopy methods may be a better choice than SRM.

We hope the practical advice in this review will help prevent possibly inaccurate and irreproducible data from being published unintentionally. Our goal is to provide information and resources to help biologists design SR experiments and save them time and frustration in the laboratory and limited financial resources. In addition, because publications are often reviewed and read by scientists who are experts in the relevant biological field but do not necessarily have expertise in every technique used in a study, we aim to provide a helpful resource to those reviewing or reading publications that use SRM.

We focus primarily on SRM methods that are commercially available and are currently the most highly represented in biology publications: single-molecule localization microscopy (SMLM; e.g., stochastic optical reconstruction microscopy [STORM], direct STORM [dSTORM], photoactivated localization microscopy [PALM], ground state depletion [GSD], and point accumulation for imaging of nanoscale topography [PAINT]), stimulated emission depletion (STED), and structured illumination microscopy (SIM; and 3D SIM). Each has been described in detail in reviews (Huang et al., 2009; Schermelleh et al., 2010; Toomre and Bewersdorf, 2010; Galbraith

and Galbraith, 2011; Eggeling et al., 2015), and we assume the reader has a basic understanding of the principles behind these techniques. Where applicable, we also discuss variants of image-scanning microscopy (ISM) methods (Sheppard, 1988; Müller and Enderlein, 2010; Sheppard et al., 2013; York et al., 2013), some of which have recently been commercialized.

Superresolution requires superoptimization

When SRM developers demonstrate the resolution of their techniques, they rigorously optimize sample preparation using their (usually custom built) microscopes, carefully correcting for sources of error. It is possible to use a commercial instrument and achieve the resolution reported by the developers (Demmerle et al., 2015), but only after learning and applying the necessary optimization procedures.

We would all like scientific discovery to come more easily. Commercial manufacturers are thus incentivized to present their SRM instruments as easy to use. But ease sometimes comes at the cost of rigor, and the SRM developers' efforts to maximize resolution and ensure accuracy in their methods are often underappreciated by the company's technical representatives, who frequently serve as researchers' primary source of information and training. Resolution reported by the SRM developers in publications and the commercial instrument manufacturers in marketing literature is usually based on the best possible results achievable under strictly limited conditions in an optimized sample. In practice, the reported SRM resolution limits are never guaranteed and do not apply to all biological samples and experiments. Careful and consistent attention to the various parameters that degrade resolution is critical to achieving optimal results.

For every diffraction-limited and SRM method, one can find an equation that defines the theoretical resolution limit of the technique (see supplement Li et al., 2015). In every case, however, there are additional practical limitations on resolution not included in these equations that, if not addressed, can decrease the achievable resolution for the particular microscope, specimen, and imaging conditions used. The practical limitations on diffraction-limited resolution have long been appreciated and include signal to noise ratio (SNR), contrast, optical aberrations, and sampling rate (Stelzer, 1998). These limitations and more apply to SRM.

SNR and contrast. SNR is the intensity of the signal of interest divided by the variance in the signal due to noise. Fluorophore choice strongly affects SNR, and fluorophores that yield sufficient signal for diffraction-limited microscopy may not provide sufficient signal for SRM. For SIM and ISM, brightness and photostability are critically important for obtaining the high SNR required for optimal reconstruction. Localization precision in SMLM is strictly dependent on SNR, as it is limited by the number of photons collected from single fluorophores (Thompson et al., 2002; Rust et al., 2006; Mortensen et al., 2010; Deschout et al., 2014). STED and SMLM additionally require fluorophores for which the transition between fluorescent and dark states can be tightly controlled during image acquisition (contrast ratio, elaborated below), and only a limited number of fluorophores fulfill both switching and brightness demands (Dempsey et al., 2011; Nahidazar et al., 2016). The importance of fluorophore choice cannot be overstated. For any SRM method, it is well worth the effort of staying up to date as better fluorescent proteins and organic dyes are developed (examples of notable recent

developments include Wurm et al., 2012; Lukinavičius et al., 2013; Shaner et al., 2013; Grimm et al., 2015).

Image contrast can be defined as the difference between the intensity of the signal of interest and the background. Out-of-focus fluorescence is a common source of background and imposes limitations on SRM. SMLM often requires the use of total internal reflection fluorescence (TIRF; Axelrod, 2001) or highly inclined and laminated optical sheet (HILO) illumination (Tokunaga et al., 2008) to reduce out-of-focus fluorescence; these methods restrict excitation and image acquisition to within a few microns of the coverslip. In SIM, both low SNR and high background can lead to artifacts. TIRF-SIM (Fiolka et al., 2008) greatly increases contrast while restricting imaging depth to ≤ 200 nm from the coverslip, whereas 3D SIM is best suited to bright samples with minimal out-of-focus fluorescence. STED and ISM microscopes typically use a pinhole to reduce the collection of out-of-focus fluorescence and may be the only viable option for thicker specimens.

Optical aberrations. Optical aberrations degrade image quality and affect resolution in diffraction-limited microscopy and SRM (Keller, 2006; Goodwin, 2007; Booth et al., 2015). The effect of aberrations on SRM can be dramatic and, if ignored, can lead to false and irreproducible results. Field- and depth-dependent aberrations have been shown to lead to SMLM localization errors as large as 50–100 nm (McGorty et al., 2014; Carlini et al., 2015; von Diezmann et al., 2015), and simulations show that aberrations can reduce SMLM localization precision twofold, introduce localization inaccuracies of many tens of nanometers, and lead to false positives (Coles et al., 2016). In STED, aberrations can increase the inner diameter of the depletion ring and/or result in depletion of emission at what should be the zero point of the depletion beam, resulting in a STED microscope that performs no better or even worse than a confocal (Deng et al., 2010; Booth et al., 2015). Aberrations may be introduced by optics (Goodwin, 2007) or the specimen (Egner and Hell, 2006). To achieve the highest resolution, microscopes must be set up to minimize aberrations for each sample. Specimens should be mounted as close as possible to the coverslip and, for fixed specimens, in a medium with a refractive index similar to coverslip glass (Goodwin, 2007). Learning to recognize and reduce aberrations is the responsibility of the microscope user because no optical system is capable of minimizing all aberrations simultaneously for all samples. We discuss two common aberrations, spherical and chromatic.

Spherical aberration is caused when light waves traveling through the periphery of a lens focus to a different plane than those passing closer to the center. Spherical aberration broadens the point spread function (PSF) both axially and laterally and decreases intensity values (Fig. 1). In SMLM, spherical aberration reduces localization precision and resolution and complicates some 3D localization methods (McGorty et al., 2014). In SIM, it decreases resolution by degrading illumination pattern contrast and raw image SNR and increases the likelihood of artifacts (Ball et al., 2015). Minimizing spherical aberration can be complicated, as it is affected by many variables: temperature, wavelength, coverslip thickness, focal plane depth, and refractive index mismatch between the lens immersion media and the specimen (North, 2006). Refractive index matching (Hiraoka et al., 1990) or objective lens correction collars (Ross et al., 2014) can be used to minimize spherical aberration for a given combination of these variables across a specific and limited range of focal depths. Spherical

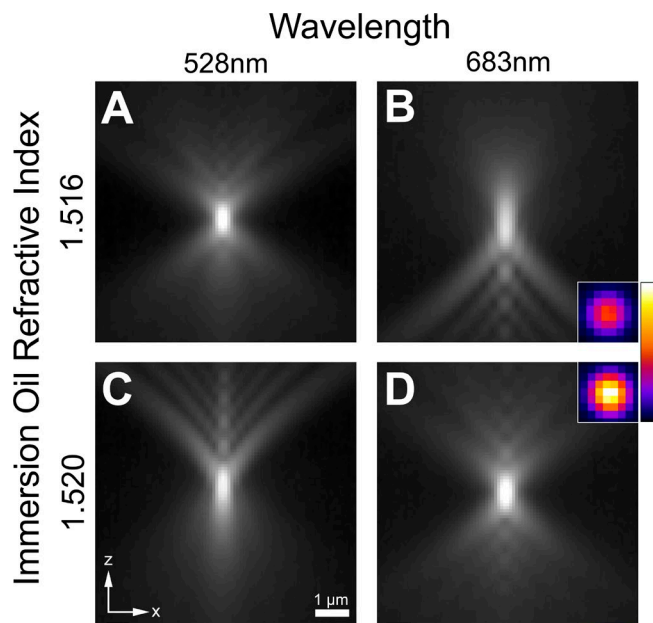


Figure 1. Spherical aberration cannot be simultaneously corrected across all wavelengths and lowers image SNR. (A–D) γ -Enhanced PSF xz views of the same multicolor fluorescent microsphere (TetraSpeck; Thermo Fisher Scientific) imaged at different emission wavelengths (528/48 nm and 683/40 nm) using different refractive index immersion oils. (A and D) Optimized PSFs are symmetric in z, with confined central maxima. (B and C) Spherical aberration results in axial asymmetry and broadening of the PSF. xy images (insets in B and D) show reduced signal intensity collected at the focal plane resulting from spherical aberration (linear intensity pseudocolored heat map displayed to the right).

aberration cannot be simultaneously corrected across multiple wavelengths (Fig. 1), so users should focus their efforts on the most important fluorophore in multichannel imaging or accept an intermediate compromise.

Chromatic aberration is a difference in focal point and lateral coordinates between wavelengths and is inherent in any optical system. Chromatic aberration must be addressed to ensure that depletion and excitation lasers are aligned in STED. Optimizing SNR in 2D and TIRF-SIM often requires using multiple cameras positioned at the different focal planes of multiple emission wavelengths. Most importantly, chromatic aberrations impose the need for postacquisition image registration for all SRM modalities (see Multiwavelength imaging section).

Fluorophore labeling density. Labeling density refers to the distance between fluorophores in a specimen. In diffraction-limited microscopy, the image of a single fluorophore is more than two orders of magnitude larger than the fluorophore, so the impact of labeling density is minimal, as even sparsely labeled structures can appear continuous. As resolution increases, inadequate labeling density can result in a confusing or misleading speckled appearance in structures that are actually continuous (Fig. 2), limiting biologically meaningful resolution. Shroff et al. (2008) explained that the distance between fluorophores must be less than half the desired resolution (Nyquist sampling; Shannon, 1949) and used simulations of various labeling densities to demonstrate this principle (also see supplement Legant et al., 2016). To achieve 20-nm resolution, for example, there must be a fluorophore bound at least every 10 nm; given the stochastic nature of probe binding, ensuring this labeling density across the field of view (FOV) can require a mean

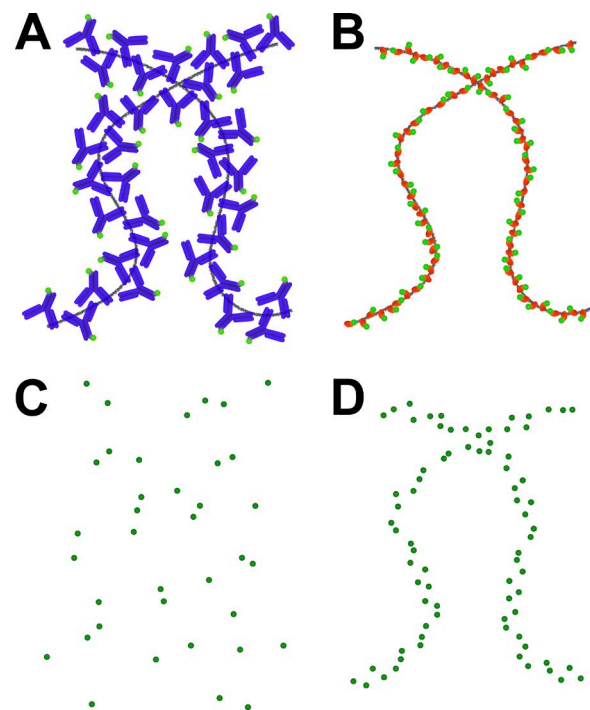


Figure 2. The effect of large probe size and low labeling density. (A) The relatively large size of antibodies can both cause steric hindrances that reduce labeling density and increase the distance between the fluorophore and the structure of interest. (B) Smaller probes may allow for higher labeling density and bring fluorophores closer to the structure of interest. (C) Inadequate labeling density can result in an ambiguous or misleading speckled appearance for structures that are actually continuous (D).

density of 5–10 \times the Nyquist rate (Legant et al., 2016). Because an IgG antibody is \sim 10 nm, reaching the labeling densities required to achieve the highest theoretical SRM resolution limits may be impossible with standard immunofluorescence protocols (Fig. 2). Using primary and fluorescently labeled secondary antibodies limits practical resolution to \geq 40 nm (Weber et al., 1978; Demmerle et al., 2015), making directly labeled primary antibodies preferable.

Labeling density requirements highlight the need for smaller probes that bind close to structures of interest, such as nanobodies (Fig. 2; Fernández-Suárez and Ting, 2008; Opazo et al., 2012; Ries et al., 2012), or imaging approaches that reduce the effect of steric hindrances. In PAINT, transient binding of freely diffusing probes can effectively increase the achievable labeling density (Sharonov and Hochstrasser, 2006). PAINT usually requires TIRF/HILO (Giannone et al., 2010) or light-sheet (Legant et al., 2016) illumination to reduce background from freely diffusing fluorophores. The number of bright target-specific PAINT probes is limited but is an active field of development (Kiuchi et al., 2015). PAINT has been used to image chromatin using fluorescently labeled oligomers (Boettiger et al., 2016), but applying similar DNA-encoded labeling strategies to protein targets (Jungmann et al., 2014) currently requires antibody intermediates.

Contrast ratio. To accurately localize molecules in SMLM, individual fluorophore emission events must be separated in time. The time a fluorophore resides in the dark versus fluorescent states (and the relative intensity of inactivated and activated forms of photoswitchable proteins) is referred to as contrast ratio. Even when labeling density requirements are

met, contrast ratio imposes limitations on attainable resolution. As sample structure and fluorophore density increase (when increased resolution is most needed), so does the probability of multiple fluorophores emitting within a diffraction-limited spot during a single exposure, which can lead to localization errors (Fig. 3). This interplay between contrast ratio and labeling density is perhaps one of the most critical and overlooked concepts in SMLM (van de Linde et al., 2010). Fluorophores do not always exhibit both high-contrast ratio and high-photon yield; organic dyes tend to be brighter than fluorescent proteins but often possess lower contrast ratios (Bates et al., 2008; Lippincott-Schwartz and Patterson, 2009; Dempsey et al., 2011). Commercially available secondary antibodies usually have many fluorophores per antibody, which reduces contrast ratio (van de Linde et al., 2010). Therefore, primary antibodies custom labeled with a mean of approximately one fluorophore are well worth the effort, as they both increase contrast ratio and bring the fluorophore closer to the target of interest.

Drift and vibration. Lateral (xy) and/or axial (z) drift within an imaging system causes the image to move or defocus over time. The magnitude of typical drift relative to resolution limits presents a bigger problem for SRM than for diffraction-limited microscopy. Drift can cause inaccuracy in SRM and introduce artifacts in SIM if it occurs during acquisition of the multiple raw images used for reconstruction. Particularly in SMLM, in which a single image can take tens of minutes to acquire, drift must be measured and corrected by using, for example, fiducial markers in the sample (Betzig et al., 2006; Rust et al., 2006). Fiducial-free drift correction algorithms exist and are included in some commercial SRM software, but their accuracy depends heavily on image content and sample structure (Huang et al., 2008; Mlodzianoski et al., 2011; Wang et al., 2014). Drift correction methods must be tested for accuracy and reproducibility. Vibration in an imaging system can reduce resolution and SNR by smearing the optical image over more pixels and can vary in frequency and magnitude over time. SR microscopes should be routinely tested for vibration, and every effort should be made to identify and remove sources (Petrak and Waters, 2014).

Estimating resolution

Given the many variables that degrade resolution, only direct measurement of the acquired SRM data can provide an estimate of the actual resolution achieved in any given experiment. Still, higher reported resolution does not always translate into visibly improved detail in images, even in images of the same structure in comparable samples (see supplement Li et al., 2015).

How can this disconnect be possible? It may arise from the fact that resolution is a deceptively intricate concept whose characterization cannot be adequately summarized using a single number (corresponding to the highest spatial frequency in an image; Li et al., 2015). Furthermore, there is no consensus on how best to estimate resolution in SRM images, and SRM developers are in active debate about the relative importance of the various factors that affect resolution (Li and Betzig, 2016; Sahl et al., 2016). All of the commonly used metrics for estimating resolution are, in some way, incomplete descriptors. We encourage researchers to estimate SRM image resolution, but with an eye toward the shortcomings of each approach, using multiple approaches when possible, and with an awareness that resolution is not constant across the FOV.

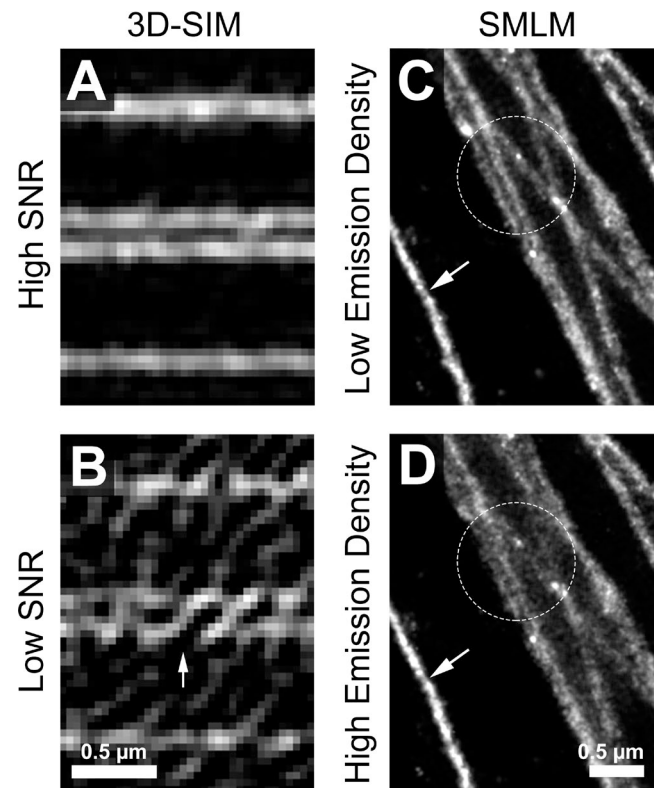


Figure 3. Common problems in SRM images. (A and B) SIM reconstructions of a standard slide (Argolight SIM) that contain continuous line structures. (A) A SIM image reconstructed from high SNR raw images closely matches the expected structures. (B) A SIM image reconstructed from low SNR raw images containing artifacts, including the appearance of structures in the background and curved lines and discontinuities, within expected structures (arrow), which were not present in the sample. For display, negative intensity values were set to 0, and images were auto-scaled. (C and D) SMLM images of Alexa Fluor 647-labeled microtubules created from datasets with lower (C) or higher (D) numbers of diffraction-limited spots that contain multiple simultaneously emitting fluorophores. The high-density dataset used to create the image in D was simulated by summing the first and second halves of the dataset in C to double the effective number of emitters in each raw image while keeping the total number of emission events constant. Molecules were localized using ThunderSTORM (single-emitter algorithm; Ovesny et al., 2014) and visualized as normalized Gaussians, with 10-nm pixel size. The presence of multiple emitters within a diffraction-limited area degrades resolution in areas of the specimen that contain higher fluorophore density, such as areas where structures overlap (circled areas). Notably, this effect is less pronounced in sparse curvilinear objects (arrows); estimating resolution using a line scan across this microtubule would misrepresent the resolution achieved elsewhere in the image.

One method commonly used to estimate resolution is to plot the intensity along a line drawn through a filamentous or punctate object in the image. The width of the intensity plot is then taken to represent the resolution achieved across the entire image. However, the specific placement of the line in the image can dramatically affect the estimate (Fig. 3) as a result of local variation in sample structure, labeling density, or background/SNR (Legant et al., 2016). With this method, multiple measurements must be made on randomly chosen structures across the entire image to reduce bias and take local variations into account.

In SMLM, localization precision is often reported but should never be interpreted as an estimate of resolution on its own. Molecular density and localization precision can be combined to calculate a lower bound on attainable resolution

(Fitzgerald et al., 2012; Legant et al., 2016), but neither alone is sufficient to fully characterize resolution, and even combined are still an incomplete descriptor as a result of additional factors such as fluorophore-linker size and sample structure (Nieuwenhuizen et al., 2013; Deschout et al., 2014).

Fourier ring correlation (FRC), commonly used in cryo-electron microscopy, has recently been applied to measure resolution in SMLM (Banterle et al., 2013; Nieuwenhuizen et al., 2013) and can easily be applied to any SRM modality. FRC requires two images of the same FOV (varying only in their noise content) or a set of SMLM localizations from the same FOV randomly divided into two. FRC provides a global estimate of resolution, does not require a priori information, and avoids bias imposed during manual placement of line scans. However, the FRC resolution estimate is heavily sample dependent; FRC can underestimate microscope performance if the underlying sample structure lacks high spatial frequency information (see supplement Legant et al., 2016). Also, FRC applied to SMLM images can yield artificially high estimates if repeated localizations of individual molecules across multiple frames are not taken into account.

Is it real, or artifact?

The promise of SRM is discernment of previously unseen spatial relationships of molecular components in biological specimens. Naturally, the question “is it real?” arises in the evaluation of SRM data. It will likely never be possible to have 100% certainty that SRM images are an accurate representation of the specimen, so it is important not to over-interpret any given feature in a single image. As with all scientific research, SRM data should be repeated over multiple experiments and specimens. Published images should be accompanied by quantitative measures describing the frequency and variability of observations. Computer-assisted image analysis can be used to reduce bias and statistical models used to calculate confidence intervals of results. We encourage healthy skepticism when viewing SRM data and awareness of the possible artifacts. We classify artifacts as intensity values or localizations in the SRM image that do not correspond to the spatial distribution of fluorophores in the specimen. Each SRM method is subject to its own potential artifacts.

SIM probably receives the most criticism for susceptibility to artifacts because of its strict dependence on computational reconstruction algorithms (Sahl et al., 2016). Indeed, great care must be taken during SIM system calibration and data acquisition to minimize reconstruction artifacts due to multiple possible sources: low SNR, background, mismatch between aberrations in raw images and the optical transfer function used for reconstruction, sample motion or photobleaching during acquisition, and illumination pattern inconsistencies across phases and rotations (Gustafsson et al., 2008; Rego and Shao, 2014; Demmerle et al., 2015). Low SNR or high background can manifest as spurious modulations of intensity (honeycomb) at spatial frequencies similar to the illumination pattern (Fig. 3), and spherical aberration mismatch can lead to axial intensity modulation (ringing) or object doubling (ghosting) and dips in intensity surrounding bright features. Users should learn to recognize these and other artifacts and modify sample preparations and/or acquisition settings to reduce them (Ball et al., 2015).

In SMLM, if two fluorophores within a diffraction-limited area fluoresce during a single exposure, algorithms that assume unimolecular emission will erroneously assign a single location

somewhere between the two molecules (Sauer, 2013). In addition to reducing resolution, this can result in artifacts in which neighboring objects appear connected or linear objects appear “webbed” at crossover points (van de Linde et al., 2010). Although relatively easy to detect in images of sparse curvilinear objects, spurious localizations are difficult to recognize in dense or unknown samples (Fig. 3). This further underscores the importance of using high-contrast ratio fluorophores. Multiemitter algorithms can improve localization precision in images with high emission density (Holden et al., 2011; Huang et al., 2011). “Missed” localizations resulting from bleaching, low SNR, and/or the acquisition of too few raw images can also be considered artifactual, as they introduce gaps or breaks not representative of the true fluorophore distribution. A “stopping criterion” for SMLM raw image acquisition could be provided by real-time localization combined with resolution metrics to evaluate when image resolution is no longer limited by localization density (Wolter et al., 2012; Nieuwenhuizen et al., 2013).

STED does not entail obligatory image processing, so it is often praised as resistant to artifacts. Indeed, STED probably is unlikely to introduce spurious image features. However, STED images often suffer from low SNR and dynamic range, which may result in missed features. Publications using STED often use postacquisition image processing, including smoothing (which reduces resolution) or deconvolution (which has the potential to introduce artifacts), to minimize the detrimental impact of low SNR.

ISM methods are also resistant to artifacts resulting from computational reconstruction, and ISM has been shown to be useful in corroborating data acquired with complementary SR methods (Nixon-Abell et al., 2016; Sivaguru et al., 2016). Nonetheless, instrument misalignment can lead to image stripping in all-optical ISM microscopes (York et al., 2013), and deconvolution during pixel reassignment is not immune to artifacts (Heintzmann et al., 2003).

In electron microscopy, preservation of ultrastructure by chemical fixation has long been a concern and a challenge. SRM can expose fixation artifacts smaller than the diffraction limit, so sample preparation protocols must be carefully validated (Halpern et al., 2015; Whelan and Bell, 2015) by looking for variation in results with different fixatives, extraction reagents, probe concentrations, and fluorophore-labeling strategies and with controls that distinguish specific from nonspecific labeling.

Standards, simulations, and software

Optimization of SRM is aided by standards for characterizing instrument performance and methods for assessing image quality. Useful standards include well-characterized biological structures (such as microtubules; Vaughan et al., 2012), nuclear pores (Löschberger et al., 2012), clathrin-coated pits (Bates et al., 2007), centrioles (Mennella et al., 2012) or synaptosomal complexes (Gustafsson et al., 2008), DNA-origami rulers (GATTQuant; Schmied et al., 2012, 2014), and micropatterned slides (Argolight). Standards help evaluate whether a given SR microscope can achieve theoretical resolution, but they do not guarantee a similar level of performance with all specimens.

Open-source software packages that provide metrics of SIM raw data and reconstruction quality (Ball et al., 2015; Křížek et al., 2016) are useful for evaluating data reproducibility, as are methods that alert users to potential artifacts (Förster et al., 2016). Bayesian reconstruction algorithms yielding estimates of local uncertainty may help validate specific SRM

image features (Orieux et al., 2012; Tang et al., 2016). Computational models and simulations have been used to evaluate whether SRM data fit with expectations based on a priori information (Rosenbloom et al., 2014; Venkataramani et al., 2016), to help guide experimental optimization (Sinkó et al., 2014), and to serve as benchmarks for the performance of various SRM reconstruction methods (Sage et al., 2015). Free and open-source SRM reconstruction algorithms are available, some of which may perform better or provide more transparency than software bundled with commercial microscopes (Deschout et al., 2014; Small and Stahlheber, 2014; Sage et al., 2015; Křížek et al., 2016; Müller et al., 2016).

Multiwavelength imaging

Multiwavelength imaging is possible with STED, SMLM, ISM, and SIM. Two-color STED (Meyer et al., 2008) is common, and three-color STED has been demonstrated (Sidenstein et al., 2016). However, the ability to acquire multiple channels depends on the available STED depletion laser, and the selection of fluorophores optimized for efficient STED depletion (Wurm et al., 2012; Kolmakov et al., 2014) rapidly dwindles as the number of desired channels increases. Multiplexing in SMLM has taken many forms, including spectrally resolved activation and reporter dyes (Bates et al., 2007; van de Linde et al., 2009), photoswitchable proteins (Shroff et al., 2007), and sequential labeling approaches (Jungmann et al., 2014; Tam et al., 2014). No two dyes have the same brightness and contrast ratio, so SMLM resolution will generally be highest in only one channel when using multiple spectral emitters (Dempsey et al., 2011; Nahidazar et al., 2016). In sequential labeling techniques such as Exchange-PAINT (Jungmann et al., 2014), buffer exchanges make drift correction critical (Dai et al., 2016). Multicolor SIM and ISM are compatible with many commonly used fluorophores, provided they are among the most bright and photostable, but resolution and SIM reconstruction quality will vary with wavelength. Aberrations are wavelength dependent (Fig. 1), and achieving optimal results across all channels in any SRM modality becomes more difficult with increasing spectral separation.

For meaningful comparisons to be made across channels, images of different wavelengths must be in perfect lateral and axial registration. Registration shifts can be introduced by chromatic aberration, by fluorescence filters that are not perfectly flat, and when multiple cameras or image-splitting devices are used. Registration errors are present to some extent in all microscopes, and registration shifts that are insignificant in diffraction-limited microscopy may be problematic in SRM. All multichannel SRM publications should report methodology and validation of channel registration.

As with any fluorescence technique, controls and corrections for bleed-through, cross talk, and autofluorescence are critical (Bolte and Cordelières, 2006). To appreciate the importance of these controls on reproducibility, see Vogel (2015). Although conventional controls are often applicable to methods like SIM, ISM, and STED, the various SMLM multiplexing approaches require different considerations, and users should familiarize themselves with the corrections required for their specific approach (for examples, see Dani et al., 2010; Bates et al., 2012; Kim et al., 2013).

To measure colocalization using SRM, it is essential to understand the nature of information provided by the method. SIM, ISM, and STED images report fluorescence intensity values,

so existing colocalization analysis methods based on overlap or intensity value correlations may often be used (Manders et al., 1993; Bolte and Cordelières, 2006). SMLM “images” do not report fluorescence intensity but are rather scatter plots of fluorophore localizations; researchers must be careful to avoid misinterpretation of SMLM data (Durisic et al., 2014). Many common image analysis methods are inapplicable to SMLM. Instead, methods that analyze localization clustering, for example, can be used to understand the distribution of one fluorophore relative to another (Barna et al., 2016; Pageon et al., 2016).

3D imaging

Although 3D SRM can attain higher axial resolution than diffraction-limited microscopy, its application is far more limited and requires compromises in imaging speed, SNR, light dose, and/or lateral resolution. Increased axial resolution in STED typically comes at the expense of lateral resolution (Klar et al., 2000). 3D SIM requires acquisition of additional images compared with 2D SIM, decreasing speed, and increasing illumination light dose. 3D SMLM methods use various PSF engineering approaches to encode depth information into 2D images (Huang et al., 2008; Juette et al., 2008; Pavani et al., 2009; Hajj et al., 2014); each approach comes with its own compromise in either lateral localization precision, axial range, or speed (Badieirostami et al., 2010). Increased axial resolution also demands increased labeling density; 20-nm resolution in three dimensions would require a minimum density of \sim 37,000 fluorophores within a 3D diffraction-limited volume (Legant et al., 2016). Because of increased complexity, it is prudent to rule out the sufficiency of 2D methods before moving to 3D.

There are inherent limitations to imaging deep into biological specimens. Biological samples have heterogeneous refractive indices and scatter and absorb light, resulting in increased aberrations and decreased SNR with distance from the coverslip (Egner and Hell, 2006). SRM is not immune to these effects and is instead particularly sensitive to aberrations and low SNR. The limitations of how deep into a sample SR can be achieved vary with different types of samples. The detection and precise localization of single molecules required for SMLM are often limited to less than a single cell layer. Thicker specimens typically also suffer from increased out-of-focus fluorescence, which degrades the quality of SIM reconstructions. The SIM illumination pattern degrades with distance from the coverslip, limiting even samples with minimal out-of-focus fluorescence to depths on the order of <20 μ m. For SRM imaging of thick specimens, thin sectioning or clearing methods may be required (Ke et al., 2016). Pinhole-based ISM methods and STED may improve contrast in thick tissues by rejecting out-of-focus fluorescence, but both are limited by light scattering with increased depth into the sample. STED has been implemented using two-photon excitation (Takasaki et al., 2013) and has also been used for *in situ* mammalian imaging (Berning et al., 2012).

Live imaging

Live-cell imaging demands deliberate navigation of the intrinsic trade-offs between spatial resolution, acquisition speed, experiment duration, and phototoxicity. Increases in spatial resolution must “borrow” from these other parameters, and we encourage readers to be mindful of these compromises when planning or evaluating live-cell SRM experiments.

Phototoxicity. Most of the cell types we image never experience a single photon *in vivo*. The possible effects of

phototoxicity on the biological process being studied must be considered and controlled for in any live-cell imaging experiment (Waters, 2007); failure to do so will almost certainly decrease the reproducibility of results. SRM must use higher illumination intensities than diffraction-limited microscopy to reach the same SNR because SRM requires that photons are collected from a smaller area of the sample and/or are distributed over more pixels (Betzig, 2015). Published SRM studies of live specimens report peak illumination intensities as high as ~5 billion times (~500 MW/cm² for STED; Lauterbach et al., 2010), ~50 million times (~5 kW/cm² for SMLM; Huang et al., 2013), and ~100 times (~10 W/cm² for SIM; Kner et al., 2009) greater than the peak solar irradiance on earth (~0.1 W/cm²). These numbers cannot be directly compared (with one another or with diffraction-limited microscopy) because the duration of illumination and the number of raw images required to generate a single SRM image vary. Regardless, the light doses used in SRM have been demonstrated to have detrimental effects and change the biological behavior of cells (Wäldchen et al., 2015). With regard to phototoxicity, Li et al. (2015) suggest that “it is prudent to start with less invasive, lower resolution methods” and move incrementally to higher resolution methods only as needed.

“Fast” live-cell SRM. Speed of image acquisition determines how accurately dynamics can be reconstructed from time-lapsed videos. Words like “fast” are used to describe some SRM modalities; this is always relative to other types of SRM and not relative to diffraction-limited microscopy, which can always acquire images faster than SRM given the same sample. Most SMLM applications require thousands to tens of thousands of images to generate a single SR image at the highest resolution. Effective acquisition rates >30 Hz have been achieved with a 169-μm² FOV (Huang et al., 2013), but with an obligatory trade-off between spatial resolution and acquisition speed (Shroff et al., 2008). Single point-scanning ISM methods (e.g., Airyscan) and STED are capable of frame rates >10–20 Hz, but point-scanning imparts trade-offs between acquisition speed, FOV, SNR, and illumination dose. Publications should be examined carefully for compromises made to achieve fast acquisition, as they are not always explicitly stated.

The modest resolution gain offered by SIM is, in a sense, its greatest strength with regard to live-cell imaging. As a wide-field technique requiring 9 (2D) to 15 (3D) images per plane, some SIM implementations can acquire FOVs >1,000 μm², at >10 frames/s, for hundreds or even thousands of time points using light doses ≤10 W/cm² (Kner et al., 2009; Li et al., 2015; Nixon-Abell et al., 2016), with the primary limitation being fluorophore brightness and detector speed. Parallelized ISM methods (e.g., instant SIM) can achieve frame rates as high as 100 Hz while maintaining illumination intensities ≤50 W/cm² and large FOV (York et al., 2013) at resolutions only slightly below conventional SIM.

Do you need SRM?

SRM has been pivotal in several biological discoveries, including determination of the structure of nuclear pores (Szymborska et al., 2013), the multimolecular arrangement of the nuclear periphery (Schermelleh et al., 2008), the stratification of focal adhesions (Kanchanawong et al., 2010), and chromatin structure across epigenetic states (Boettiger et al., 2016). We have seen our core facility users obtain results with SRM that would not have been possible with diffraction-limited techniques.

However, SRM is currently (for lack of a better word) trendy, and the perception exists that inclusion of an SRM figure increases the likelihood of publication of a research study. We encourage researchers to use SRM only when it is the best tool for the question at hand. The complexity and compromises in SRM make diffraction-limited microscopy preferable wherever appropriate. Even when imaging structures smaller than the diffraction limit, SRM is not necessarily the best choice. Before turning to SRM, it is important to differentiate between the need for increased resolution and the need for sensitivity, contrast, and/or quantitative image analysis.

Or do you need sensitivity? Detection of objects reveals their presence, whereas resolution allows closely spaced objects to be distinguished as separate from one another in the image. Sensitivity is required to detect features in the specimen that emit fewer photons. Diffraction-limited microscopes can be used very effectively for applications that require the highest possible sensitivity; they are, for example, routinely used for single-molecule imaging. SRM methods are not inherently more sensitive than diffraction-limited microscopy and are far less sensitive in some applications. If you are struggling to detect fluorescence in your sample, focus your efforts on increasing the sensitivity of your diffraction-limited microscope (Murray et al., 2007; Waters, 2009). SRM is most appropriate when the features of interest are detectable with diffraction-limited microscopy but are too densely distributed to be resolved. Structures that appear only in SRM images may be artifacts or the result of a poorly performing diffraction-limited microscope.

Or do you need contrast? SRM methods often result in high-contrast images as a result of either rejection of out-of-focus fluorescence (STED and ISM), postacquisition processing (SIM and ISM), or display (SMLM). Contrast is visually appealing but different from resolution. Out-of-focus fluorescence, autofluorescence, excess fluorophores, or excitation light leaking through filter sets can all reduce contrast and should be addressed directly. Optical sectioning techniques such as confocal, HILo, TIRF, and light sheet can dramatically decrease out-of-focus fluorescence in diffraction-limited images (Axelrod, 2001; Conchello and Lichtman, 2005; Tokunaga et al., 2008; Weber et al., 2014). When SRM images are displayed next to hazy diffraction-limited images and the scale bar reveals that the “now-resolved” structures are separated by more than the diffraction limit, it was likely contrast—not resolution—that was originally lacking.

Or do you need image analysis? The human brain is exquisitely tuned to visual information. The phrase “seeing is believing” reflects the emphasis placed on qualitatively demonstrating a particular concept with images. However, computer-assisted quantitative analysis can reveal information that cannot be seen by eye. Using diffraction-limited images, precise measurements can be made of distances and phenomena that occur far below the diffraction limit (Verdaasdonk et al., 2014) with higher temporal resolution and far lower light doses than any SRM method. Gaussian fitting can be used to track the movement of isolated diffraction-limited objects with nanometer precision (Gelles et al., 1988; Yildiz et al., 2003). Spectral (Lacoste et al., 2000) and temporal (Gordon et al., 2004; Qu et al., 2004) information can also be exploited to discriminate objects spaced well below the diffraction limit. For example, using diffraction-limited microscopy with image analysis, Churchman et al. (2005) measured distances between two different

fluorophores bound to the same myosin V macromolecule, and Joglekar et al. (2006) determined the relative positions of eight kinetochore multiprotein complexes with 10-nm resolution. Sometimes, a change in labeling strategy can reveal new information: sparse fluorescent labeling (fluorescent speckle microscopy) has been used to quantify otherwise unresolvable cytoskeletal dynamics with statistical power that would have been impossible with SRM (Danuser and Waterman-Storer, 2006). Counting the number of molecules/objects in a sample does not always require resolving individual molecules/objects. Accurate counting has been achieved through quantitative image analysis of fluorescence intensities using diffraction-limited microscopy (Wu and Pollard, 2005; Joglekar et al., 2006; Lu et al., 2015).

Summary

Careful attention must be paid to sample preparation methods, image acquisition parameters, correction for aberrations, and the possibility of artifacts to ensure accurate and reproducible SRM results. SR microscopes should be routinely characterized and optimized using standard test samples to ensure they are performing as expected. Computational image analysis and/or simulations should be used to validate SRM results. While undoubtedly an impressive set of technologies, SRM is also more difficult and in every way except resolution more limited than diffraction-limited microscopy, so SRM should be preferred only when diffraction-limited methods will not suffice. With the same rigorous attention to detail demonstrated by SRM developers, we expect biologists will continue to leverage SRM to make exciting advances in our understanding of cellular and molecular structure and function.

Acknowledgments

The authors thank the faculty and students of the Quantitative Imaging course (Cold Spring Harbor Laboratory) for many enthusiastic discussions and Jessica Tytell and Anna Payne-Tobin Jost for insightful comments.

The authors declare no competing financial interests.

Submitted: 5 October 2016

Revised: 15 November 2016

Accepted: 18 November 2016

References

Axelrod, D. 2001. Total internal reflection fluorescence microscopy in cell biology. *Traffic*. 2:764–774. <http://dx.doi.org/10.1034/j.1600-0854.2001.21104.x>

Badicrostami, M., M.D. Lew, M.A. Thompson, and W.E. Moerner. 2010. Three-dimensional localization precision of the double-helix point spread function versus astigmatism and biplane. *Appl. Phys. Lett.* 97:161103. <http://dx.doi.org/10.1063/1.3499652>

Ball, G., J. Demmerle, R. Kaufmann, I. Davis, I.M. Dobbie, and L. Schermelleh. 2015. SIMcheck: a toolbox for successful super-resolution structured illumination microscopy. *Sci. Rep.* 5:15915. <http://dx.doi.org/10.1038/srep15915>

Banterle, N., K.H. Bui, E.A. Lemke, and M. Beck. 2013. Fourier ring correlation as resolution criterion for super-resolution microscopy. *J. Struct. Biol.* 183:363–367. <http://dx.doi.org/10.1016/j.jsb.2013.05.004>

Barna, L., B. Dudok, V. Miczán, A. Horváth, Z.I. László, and I. Katona. 2016. Correlated confocal and super-resolution imaging by VividSTORM. *Nat. Protoc.* 11:163–183. <http://dx.doi.org/10.1038/nprot.2016.002>

Bates, M., B. Huang, G.T. Dempsey, and X. Zhuang. 2007. Multicolor super-resolution imaging with photo-switchable fluorescent probes. *Science*. 317:1749–1753. <http://dx.doi.org/10.1126/science.1146598>

Bates, M., B. Huang, and X. Zhuang. 2008. Super-resolution microscopy by nanoscale localization of photo-switchable fluorescent probes. *Curr. Opin. Chem. Biol.* 12:505–514. <http://dx.doi.org/10.1016/j.cbpa.2008.08.008>

Bates, M., G.T. Dempsey, K.H. Chen, and X. Zhuang. 2012. Multicolor super-resolution fluorescence imaging via multi-parameter fluorophore detection. *ChemPhysChem*. 13:99–107. <http://dx.doi.org/10.1002/cphc.201100735>

Berning, S., K.I. Willig, H. Steffens, P. Dibaj, and S.W. Hell. 2012. Nanoscopy in a living mouse brain. *Science*. 335:551. <http://dx.doi.org/10.1126/science.1215369>

Betzig, E. 2015. Single molecules, cells, and super-resolution optics (Nobel lecture). *Angew. Chem. Int. Ed. Engl.* 54:8034–8053. <http://dx.doi.org/10.1002/anie.201501003>

Betzig, E., G.H. Patterson, R. Sougrat, O.W. Lindwasser, S. Olenych, J.S. Bonifacino, M.W. Davidson, J. Lippincott-Schwartz, and H.F. Hess. 2006. Imaging intracellular fluorescent proteins at nanometer resolution. *Science*. 313:1642–1645. <http://dx.doi.org/10.1126/science.1127344>

Boettiger, A.N., B. Bintu, J.R. Moffitt, S. Wang, B.J. Beliveau, G. Fudenberg, M. Imakaev, L.A. Mirny, C.-T. Wu, and X. Zhuang. 2016. Super-resolution imaging reveals distinct chromatin folding for different epigenetic states. *Nature*. 529:418–422. <http://dx.doi.org/10.1038/nature16496>

Bolte, S., and F.P. Cordelieres. 2006. A guided tour into subcellular colocalization analysis in light microscopy. *J. Microsc.* 224:213–232. <http://dx.doi.org/10.1111/j.1365-2818.2006.01706.x>

Booth, M., D. Andrade, D. Burke, B. Patton, and M. Zurauskas. 2015. Aberrations and adaptive optics in super-resolution microscopy. *Microscopy (Oxf.)*. 64:251–261. <http://dx.doi.org/10.1093/micro/dvfv033>

Carlini, L., S.J. Holden, K.M. Douglass, and S. Manley. 2015. Correction of a depth-dependent lateral distortion in 3D super-resolution imaging. *PLoS One*. 10. <http://dx.doi.org/10.1371/journal.pone.0142949>

Churchman, L.S., Z. Ökten, and R.S. Rock. 2005. Single molecule high-resolution colocalization of Cy3 and Cy5 attached to macromolecules measures intramolecular distances through time. *Proc. Natl. Acad. Sci. USA*. 102:1419–1423.

Coles, B.C., S.E.D. Webb, N. Schwartz, D.J. Rolfe, M. Martin-Fernandez, and V. Lo Schiavo. 2016. Characterisation of the effects of optical aberrations in single molecule techniques. *Biomed. Opt. Express*. 7:1755–1767. <http://dx.doi.org/10.1364/BOE.7.001755>

Conchello, J.-A., and J.W. Lichtman. 2005. Optical sectioning microscopy. *Nat. Methods*. 2:920–931. <http://dx.doi.org/10.1038/nmeth1815>

Dai, M., R. Jungmann, and P. Yin. 2016. Optical imaging of individual biomolecules in densely packed clusters. *Nat. Nanotechnol.* 11:798–807. <http://dx.doi.org/10.1038/nnano.2016.95>

Dani, A., B. Huang, J. Bergan, C. Dulac, and X. Zhuang. 2010. Superresolution imaging of chemical synapses in the brain. *Neuron*. 68:843–856. <http://dx.doi.org/10.1016/j.neuron.2010.11.021>

Danuser, G., and C.M. Waterman-Storer. 2006. Quantitative fluorescent speckle microscopy of cytoskeleton dynamics. *Annu. Rev. Biophys. Biomol. Struct.* 35:361–387. <http://dx.doi.org/10.1146/annurev.biophys.35.040405.102114>

Demmerle, J., E. Wegel, L. Schermelleh, and I.M. Dobbie. 2015. Assessing resolution in super-resolution imaging. *Methods*. 88:3–10. <http://dx.doi.org/10.1016/j.ymeth.2015.07.001>

Dempsey, G.T., J.C. Vaughan, K.H. Chen, M. Bates, and X. Zhuang. 2011. Evaluation of fluorophores for optimal performance in localization-based super-resolution imaging. *Nat. Methods*. 8:1027–1036. <http://dx.doi.org/10.1038/nmeth.1768>

Deng, S., L. Liu, Y. Cheng, R. Li, and Z. Xu. 2010. Effects of primary aberrations on the fluorescence depletion patterns of STED microscopy. *Opt. Express*. 18:1657–1666. <http://dx.doi.org/10.1364/OE.18.001657>

Deschout, H., F. Cella Zanacchi, M. Mlodzianoski, A. Diaspro, J. Bewersdorf, S.T. Hess, and K. Braeckmans. 2014. Precisely and accurately localizing single emitters in fluorescence microscopy. *Nat. Methods*. 11:253–266. <http://dx.doi.org/10.1038/nmeth.2843>

Durisic, N., L.L. Cuervo, and M. Lakadamyali. 2014. Quantitative super-resolution microscopy: pitfalls and strategies for image analysis. *Curr. Opin. Chem. Biol.* 20:22–28. <http://dx.doi.org/10.1016/j.cbpa.2014.04.005>

Eggeling, C., K.I. Willig, S.J. Sahl, and S.W. Hell. 2015. Lens-based fluorescence nanoscopy. *Q. Rev. Biophys.* 48:178–243. <http://dx.doi.org/10.1017/S003583514000146>

Egner, A., and S.W. Hell. 2006. Aberrations in confocal and multi-photon fluorescence microscopy induced by refractive index mismatch. In *Handbook of Biological Confocal Microscopy*. J.B. Pawley, editor. Springer US, Boston, MA. 404–413. http://dx.doi.org/10.1007/978-0-387-45524-2_20

Fernández-Suárez, M., and A.Y. Ting. 2008. Fluorescent probes for super-resolution imaging in living cells. *Nat. Rev. Mol. Cell Biol.* 9:929–943. <http://dx.doi.org/10.1038/nrm2531>

Fiolka, R., M. Beck, and A. Stemmer. 2008. Structured illumination in total internal reflection fluorescence microscopy using a spatial light modulator. *Opt. Lett.* 33:1629–1631. <http://dx.doi.org/10.1364/OL.33.001629>

Fitzgerald, J.E., J. Lu, and M.J. Schnitzer. 2012. Estimation theoretic measure of resolution for stochastic localization microscopy. *Phys. Rev. Lett.* 109:048102. <http://dx.doi.org/10.1103/PhysRevLett.109.048102>

Förster, R., K. Wicker, W. Müller, A. Jost, and R. Heintzmann. 2016. Motion artefact detection in structured illumination microscopy for live cell imaging. *Opt. Express.* 24:22121–22134. <http://dx.doi.org/10.1364/OE.24.022121>

Galbraith, C.G., and J.A. Galbraith. 2011. Super-resolution microscopy at a glance. *J. Cell Sci.* 124:1607–1611. <http://dx.doi.org/10.1242/jcs.080085>

Gelles, J., B.J. Schnapp, and M.P. Sheetz. 1988. Tracking kinesin-driven movements with nanometre-scale precision. *Nature*. 331:450–453. <http://dx.doi.org/10.1038/331450a0>

Giannone, G., E. Hosy, F. Levet, A. Constals, K. Schulze, A.I. Sobolevsky, M.P. Rosconi, E. Gouaux, R. Tampé, D. Choquet, and L. Cognet. 2010. Dynamic superresolution imaging of endogenous proteins on living cells at ultra-high density. *Biophys. J.* 99:1303–1310. <http://dx.doi.org/10.1016/j.bpj.2010.06.005>

Goodwin, P.C. 2007. Evaluating optical aberration using fluorescent microspheres: Methods, analysis, and corrective actions. In *Digital Microscopy*. Third edition. Vol. 81. G. Sluder and D.E. Wolf, editors. Elsevier, Amsterdam. 397–413. [http://dx.doi.org/10.1016/S0091-679X\(06\)81018-6](http://dx.doi.org/10.1016/S0091-679X(06)81018-6)

Gordon, M.P., T. Ha, and P.R. Selvin. 2004. Single-molecule high-resolution imaging with photobleaching. *Proc. Natl. Acad. Sci. USA*. 101:6462–6465. <http://dx.doi.org/10.1073/pnas.0401638101>

Grimm, J.B., B.P. English, J. Chen, J.P. Slaughter, Z. Zhang, A. Revyakin, R. Patel, J.J. Macklin, D. Normanno, R.H. Singer, et al. 2015. A general method to improve fluorophores for live-cell and single-molecule microscopy. *Nat. Methods*. 12:244–250; 3: 250. <http://dx.doi.org/10.1038/nmeth.3256>

Gustafsson, M.G., L. Shao, P.M. Carlton, C.J.R. Wang, I.N. Golubovskaya, W.Z. Cande, D.A. Agard, and J.W. Sedat. 2008. Three-dimensional resolution doubling in wide-field fluorescence microscopy by structured illumination. *Biophys. J.* 94:4957–4970. <http://dx.doi.org/10.1529/biophys.107.120345>

Hajj, B., M. El Beheiry, I. Izeddin, X. Darzacq, and M. Dahan. 2014. Accessing the third dimension in localization-based super-resolution microscopy. *Phys. Chem. Chem. Phys.* 16:16340–16348. <http://dx.doi.org/10.1039/C4CP01380H>

Halpern, A.R., M.D. Howard, and J.C. Vaughan. 2015. Point by point: An introductory guide to sample preparation for single-molecule, super-resolution fluorescence microscopy. *Curr. Protoc. Chem. Biol.* 7:103–120. <http://dx.doi.org/10.1002/9780470559277.ch140241>

Heintzmann, R., V. Sarafis, P. Munroe, J. Nailon, Q.S. Hanley, and T.M. Jovin. 2003. Resolution enhancement by subtraction of confocal signals taken at different pinhole sizes. *Micron*. 34:293–300. [http://dx.doi.org/10.1016/S0968-4328\(03\)00054-4](http://dx.doi.org/10.1016/S0968-4328(03)00054-4)

Hiraoka, Y., J.W. Sedat, and D.A. Agard. 1990. Determination of three-dimensional imaging properties of a light microscope system. Partial confocal behavior in epifluorescence microscopy. *Biophys. J.* 57:325–333. [http://dx.doi.org/10.1016/S0006-3495\(90\)82534-0](http://dx.doi.org/10.1016/S0006-3495(90)82534-0)

Holden, S.J., S. Uphoff, and A.N. Kapanidis. 2011. DAOSTORM: an algorithm for high-density super-resolution microscopy. *Nat. Methods*. 8:279–280. <http://dx.doi.org/10.1038/nmeth0411-279>

Huang, B., W. Wang, M. Bates, and X. Zhuang. 2008. Three-dimensional super-resolution imaging by stochastic optical reconstruction microscopy. *Science*. 319:810–813. <http://dx.doi.org/10.1126/science.1153529>

Huang, B., M. Bates, and X. Zhuang. 2009. Super-resolution fluorescence microscopy. *Annu. Rev. Biochem.* 78:993–1016. <http://dx.doi.org/10.1146/annurev.biochem.77.061906.092014>

Huang, F., S.L. Schwartz, J.M. Byars, and K.A. Lidke. 2011. Simultaneous multiple-emitter fitting for single molecule super-resolution imaging. *Biomed. Opt. Express.* 2:1377–1393. <http://dx.doi.org/10.1364/BOE.2.001377>

Huang, F., T.M.P. Hartwich, F.E. Rivera-Molina, Y. Lin, W.C. Duim, J.J. Long, P.D. Uchil, J.R. Myers, M.A. Baird, W. Mothes, et al. 2013. Video-rate nanoscopy using sCMOS camera-specific single-molecule localization algorithms. *Nat. Methods*. 10:653–658. <http://dx.doi.org/10.1038/nmeth.2488>

Joglekar, A.P., D.C. Bouck, J.N. Molk, K.S. Bloom, and E.D. Salmon. 2006. Molecular architecture of a kinetochore-microtubule attachment site. *Nat. Cell Biol.* 8:581–585. <http://dx.doi.org/10.1038/nccb1414>

Juette, M.F., T.J. Gould, M.D. Lessard, M.J. Mlodzianoski, B.S. Nagpure, B.T. Bennett, S.T. Hess, and J. Bewersdorf. 2008. Three-dimensional sub-100 nm resolution fluorescence microscopy of thick samples. *Nat. Methods*. 5:527–529. <http://dx.doi.org/10.1038/nmeth.1211>

Jungmann, R., M.S. Avendaño, J.B. Woehrstein, M. Dai, W.M. Shih, and P. Yin. 2014. Multiplexed 3D cellular super-resolution imaging with DNA-PAINT and Exchange-PAINT. *Nat. Methods*. 11:313–318. <http://dx.doi.org/10.1038/nmeth.2835>

Kanchanawong, P., G. Shtengel, A.M. Pasapera, E.B. Ramko, M.W. Davidson, H.F. Hess, and C.M. Waterman. 2010. Nanoscale architecture of integrin-based cell adhesions. *Nature*. 468:580–584. <http://dx.doi.org/10.1038/nature09621>

Ke, M.-T., Y. Nakai, S. Fujimoto, R. Takayama, S. Yoshida, T.S. Kitajima, M. Sato, and T. Imai. 2016. Super-resolution mapping of neuronal circuitry with an index-optimized clearing agent. *Cell Reports*. 14:2718–2732. <http://dx.doi.org/10.1016/j.celrep.2016.02.057>

Keller, H.E. 2006. Objective lenses for confocal microscopy. In *Handbook of Biological Confocal Microscopy*. Springer-Verlag New York Inc., New York. 145–161. http://dx.doi.org/10.1007/978-0-387-45524-2_7

Kim, D., N.M. Curthoys, M.T. Parent, and S.T. Hess. 2013. Bleed-through correction for rendering and correlation analysis in multi-colour localization microscopy. *J. Opt.* 15:094011. <http://dx.doi.org/10.1088/2040-8978/15/9/094011>

Kiuchi, T., M. Higuchi, A. Takamura, M. Maruoka, and N. Watanabe. 2015. Multitarget super-resolution microscopy with high-density labeling by exchangeable probes. *Nat. Methods*. 12:743–746. <http://dx.doi.org/10.1038/nmeth.3466>

Klar, T.A., S. Jakobs, and M. Dyba. 2000. Fluorescence microscopy with diffraction resolution barrier broken by stimulated emission. *Proc. Natl. Acad. Sci. USA*. 97:8206–8210.

Kner, P., B.B. Chhun, E.R. Griffis, L. Winoto, and M.G. Gustafsson. 2009. Super-resolution video microscopy of live cells by structured illumination. *Nat. Methods*. 6:339–342. <http://dx.doi.org/10.1038/nmeth.1324>

Kolmakov, K., C.A. Wurm, D.N.H. Meineke, F. Göttfert, V.P. Boyarskiy, V.N. Belov, and S.W. Hell. 2014. Polar red-emitting rhodamine dyes with reactive groups: synthesis, photophysical properties, and two-color STED nanoscopy applications. *Chemistry*. 20:146–157. <http://dx.doi.org/10.1002/chem.201303433>

Křížek, P., T. Lukeš, M. Ovesný, K. Fliegel, and G.M. Hagen. 2016. SIMToolbox: a MATLAB toolbox for structured illumination fluorescence microscopy. *Bioinformatics*. 32:318–320. <http://dx.doi.org/10.1093/bioinformatics/btv576>

Lacoste, T.D., X. Michalet, F. Pinaud, D.S. Chemla, A.P. Alivisatos, and S. Weiss. 2000. Ultrahigh-resolution multicolor colocalization of single fluorescent probes. *Proc. Natl. Acad. Sci. USA*. 97:9461–9466. <http://dx.doi.org/10.1073/pnas.170286097>

Lauterbach, M.A., J. Keller, A. Schönle, D. Kamin, V. Westphal, S.O. Rizzoli, and S.W. Hell. 2010. Comparing video-rate STED nanoscopy and confocal microscopy of living neurons. *J. Biophotonics*. 3:417–424. <http://dx.doi.org/10.1002/jbio.201000038>

Legant, W.R., L. Shao, J.B. Grimm, T.A. Brown, D.E. Milkie, B.B. Avants, L.D. Lavis, and E. Betzig. 2016. High-density three-dimensional localization microscopy across large volumes. *Nat. Methods*. 13:359–365. <http://dx.doi.org/10.1038/nmeth.3797>

Li, D., and E. Betzig. 2016. Response to comment on “Extended-resolution structured illumination imaging of endocytic and cytoskeletal dynamics”. *Science*. 352:527. <http://dx.doi.org/10.1126/science.aad8396>

Li, D., L. Shao, B.-C. Chen, X. Zhang, M. Zhang, B. Moses, D.E. Milkie, J.R. Beach, J.A. Hammer III, M. Pasham, et al. 2015. Extended-resolution structured illumination imaging of endocytic and cytoskeletal dynamics. *Science*. 349. <http://dx.doi.org/10.1126/science.aab3500>

Lippincott-Schwartz, J., and G.H. Patterson. 2009. Photoactivatable fluorescent proteins for diffraction-limited and super-resolution imaging. *Trends Cell Biol.* 19:555–565. <http://dx.doi.org/10.1016/j.tcb.2009.09.003>

Löschberger, A., S. van de Linde, M.-C. Dabauvalle, B. Rieger, M. Heilemann, G. Krohne, and M. Sauer. 2012. Super-resolution imaging visualizes the eightfold symmetry of gp210 proteins around the nuclear pore complex and resolves the central channel with nanometer resolution. *J. Cell Sci.* 125:570–575. <http://dx.doi.org/10.1242/jcs.098822>

Lu, Y., B.-H. Lee, R.W. King, D. Finley, and M.W. Kirschner. 2015. Substrate degradation by the proteasome: a single-molecule kinetic analysis. *Science*. 348. <http://dx.doi.org/10.1126/science.1250834>

Lukinavičius, G., K. Umezawa, N. Olivier, A. Honigmann, G. Yang, T. Plass, V. Mueller, L. Reymond, I.R. Corrêa Jr., Z.-G. Luo, et al. 2013. A near-infrared fluorophore for live-cell super-resolution microscopy of cellular proteins. *Nat. Chem.* 5:132–139. <http://dx.doi.org/10.1038/nchem.1546>

Manders, E.M.M., F.J. Verbeek, and J.A. Aten. 1993. Measurement of co-localization of objects in dual-colour confocal images. *J. Microsc.* 169:375–382. <http://dx.doi.org/10.1111/j.1365-2818.1993.tb03313.x>

McGorty, R., J. Schnitzbauer, W. Zhang, and B. Huang. 2014. Correction of depth-dependent aberrations in 3D single-molecule localization and super-resolution microscopy. *Opt. Lett.* 39:275–278. <http://dx.doi.org/10.1364/OL.39.000275>

Mennella, V., B. Keszthelyi, K.L. McDonald, B. Chhun, F. Kan, G.C. Rogers, B. Huang, and D.A. Agard. 2012. Subdiffraction-resolution fluorescence microscopy reveals a domain of the centrosome critical for pericentriolar material organization. *Nat. Cell Biol.* 14:1159–1168. <http://dx.doi.org/10.1038/ncb2597>

Meyer, L., D. Wildanger, R. Medda, A. Punge, S.O. Rizzoli, G. Donnert, and S.W. Hell. 2008. Dual-color STED microscopy at 30-nm focal-plane resolution. *Small.* 4:1095–1100. <http://dx.doi.org/10.1002/smll.200800055>

Mlodzianoski, M.J., J.M. Schreiner, S.P. Callahan, K. Smolková, A. Dlasková, J. Santorová, P. Ježek, and J. Bewersdorf. 2011. Sample drift correction in 3D fluorescence photoactivation localization microscopy. *Opt. Express.* 19:15009–15019. <http://dx.doi.org/10.1364/OE.19.015009>

Mortensen, K.I., L.S. Churchman, J.A. Spudich, and H. Flyvbjerg. 2010. Optimized localization analysis for single-molecule tracking and super-resolution microscopy. *Nat. Methods.* 7:377–381. <http://dx.doi.org/10.1038/nmeth.1447>

Müller, C.B., and J. Enderlein. 2010. Image scanning microscopy. *Phys. Rev. Lett.* 104:198101. <http://dx.doi.org/10.1103/PhysRevLett.104.198101>

Müller, M., V. Mönkemöller, S. Hennig, W. Hübner, and T. Huser. 2016. Open-source image reconstruction of super-resolution structured illumination microscopy data in ImageJ. *Nat. Commun.* 7:10980. <http://dx.doi.org/10.1038/ncomms10980>

Murray, J.M., P.L. Appleton, J.R. Swedlow, and J.C. Waters. 2007. Evaluating performance in three-dimensional fluorescence microscopy. *J. Microsc.* 228:390–405. <http://dx.doi.org/10.1111/j.1365-2818.2007.01861.x>

Nahidiziar, L., A.V. Agronskaia, J. Broertjes, B. van den Broek, and K. Jalink. 2016. Optimizing imaging conditions for demanding multi-color super resolution localization microscopy. *PLoS One.* 11. <http://dx.doi.org/10.1371/journal.pone.0158884>

Nieuwenhuizen, R.P.J., K.A. Lidke, M. Bates, D.L. Puig, D. Grünwald, S. Stallinga, and B. Rieger. 2013. Measuring image resolution in optical nanoscopy. *Nat. Methods.* 10:557–562. <http://dx.doi.org/10.1038/nmeth.2448>

Nixon-Abell, J., C.J. Obara, A.V. Weigel, D. Li, W.R. Legant, C.S. Xu, H.A. Pasolli, K. Harvey, H.F. Hess, E. Betzig, et al. 2016. Increased spatiotemporal resolution reveals highly dynamic dense tubular matrices in the peripheral ER. *Science*. 354. <http://dx.doi.org/10.1126/science.aaf3928>

North, A.J. 2006. Seeing is believing? A beginners' guide to practical pitfalls in image acquisition. *J. Cell Biol.* 172:9–18. <http://dx.doi.org/10.1083/jcb.200507103>

Opazo, F., M. Levy, M. Byrom, C. Schäfer, C. Geisler, T.W. Groemer, A.D. Ellington, and S.O. Rizzoli. 2012. Aptamers as potential tools for super-resolution microscopy. *Nat. Methods.* 9:938–939. <http://dx.doi.org/10.1038/nmeth.2179>

Orieux, F., E. Sepulveda, V. Lorette, B. Dubertret, and J.-C. Olivo-Marin. 2012. Bayesian estimation for optimized structured illumination microscopy. *IEEE Trans. Image Process.* 21:601–614. <http://dx.doi.org/10.1109/TIP.2011.2162741>

Ovesný, M., P. Krížek, J. Borkovec, Z. Švindrych, and G.M. Hagen. 2014. ThunderSTORM: a comprehensive ImageJ plug-in for PALM and STORM data analysis and super-resolution imaging. *Bioinformatics*. 30:2389–2390. <http://dx.doi.org/10.1093/bioinformatics/btu202>

Pageon, S.V., P.R. Nicovich, M. Mollazade, T. Tabarin, and K. Gaus. 2016. ClusDoC: a combined cluster detection and colocalization analysis for single-molecule localization microscopy data. *Mol. Biol. Cell.* 27:3627–3636. <http://dx.doi.org/10.1091/mbc.E16-07-0478>

Pavani, S.R.P., M.A. Thompson, J.S. Biteen, S.J. Lord, N. Liu, R.J. Twieg, R. Piestun, and W.E. Moerner. 2009. Three-dimensional, single-molecule fluorescence imaging beyond the diffraction limit by using a double-helix point spread function. *Proc. Natl. Acad. Sci. USA.* 106:2995–2999. <http://dx.doi.org/10.1073/pnas.0900245106>

Petrak, L.J., and J.C. Waters. 2014. A practical guide to microscope care and maintenance. *Methods Cell Biol.* 123:55–76. <http://dx.doi.org/10.1016/B978-0-12-420138-5.00004-5>

Qu, X., D. Wu, L. Mets, and N.F. Scherer. 2004. Nanometer-localized multiple single-molecule fluorescence microscopy. *Proc. Natl. Acad. Sci. USA.* 101:11298–11303. <http://dx.doi.org/10.1073/pnas.0402155101>

Rego, E.H., and L. Shao. 2014. Practical structured illumination microscopy. In *Advanced Fluorescence Microscopy*. P.J. Verveer, editor. Springer-Verlag New York Inc., NY. 175–192.

Ries, J., C. Kaplan, E. Platonova, H. Eghlidi, and H. Ewers. 2012. A simple, versatile method for GFP-based super-resolution microscopy via nanobodies. *Nat. Methods.* 9:582–584. <http://dx.doi.org/10.1038/nmeth.1991>

Rosenbloom, A.B., S.-H. Lee, M. To, A. Lee, J.Y. Shin, and C. Bustamante. 2014. Optimized two-color super resolution imaging of Drp1 during mitochondrial fission with a slow-switching Dronpa variant. *Proc. Natl. Acad. Sci. USA.* 111:13093–13098. <http://dx.doi.org/10.1073/pnas.1320044111>

Ross, S.T., J.R. Allen, and M.W. Davidson. 2014. Practical considerations of objective lenses for application in cell biology. *Methods Cell Biol.* 123:19–34. <http://dx.doi.org/10.1016/B978-0-12-420138-5.00002-1>

Rust, M.J., M. Bates, and X. Zhuang. 2006. Sub-diffraction-limit imaging by stochastic optical reconstruction microscopy (STORM). *Nat. Methods.* 3:793–796. <http://dx.doi.org/10.1038/nmeth929>

Sage, D., H. Kirshner, T. Pengo, N. Stuurman, J. Min, S. Manley, and M. Unser. 2015. Quantitative evaluation of software packages for single-molecule localization microscopy. *Nat. Methods.* 12:717–724. <http://dx.doi.org/10.1038/nmeth.3442>

Sahl, S.J., F. Balzarotti, J. Keller-Findeisen, M. Leutenegger, V. Westphal, A. Egner, F. Lavoie-Cardinal, A. Chmyrov, T. Grotjohann, and S. Jakobs. 2016. Comment on “Extended-resolution structured illumination imaging of endocytic and cytoskeletal dynamics”. *Science*. 352:527. <http://dx.doi.org/10.1126/science.aad7983>

Sauer, M. 2013. Localization microscopy coming of age: from concepts to biological impact. *J. Cell Sci.* 126:3505–3513. <http://dx.doi.org/10.1242/jcs.123612>

Schermelleh, L., P.M. Carlton, S. Haase, L. Shao, L. Winoto, P. Kner, B. Burke, M.C. Cardoso, D.A. Agard, M.G. Gustafsson, et al. 2008. Subdiffraction multicolor imaging of the nuclear periphery with 3D structured illumination microscopy. *Science*. 320:1332–1336. <http://dx.doi.org/10.1126/science.1156947>

Schermelleh, L., R. Heintzmann, and H. Leonhardt. 2010. A guide to super-resolution fluorescence microscopy. *J. Cell Biol.* 190:165–175. <http://dx.doi.org/10.1083/jcb.201002018>

Schmid, J.J., A. Gietl, P. Holzmeister, C. Forthmann, C. Steinhauer, T. Dammeyer, and P. Tinnefeld. 2012. Fluorescence and super-resolution standards based on DNA origami. *Nat. Methods.* 9:1133–1134. <http://dx.doi.org/10.1038/nmeth.2254>

Schmid, J.J., M. Raab, C. Forthmann, E. Pibiri, B. Wünsch, T. Dammeyer, and P. Tinnefeld. 2014. DNA origami-based standards for quantitative fluorescence microscopy. *Nat. Protoc.* 9:1367–1391. <http://dx.doi.org/10.1038/nprot.2014.079>

Shaner, N.C., G.G. Lambert, A. Chammas, Y. Ni, P.J. Cranfill, M.A. Baird, B.R. Sell, J.R. Allen, R.N. Day, M. Israelsson, et al. 2013. A bright monomeric green fluorescent protein derived from *Branchiostoma lanceolatum*. *Nat. Methods.* 10:407–409. <http://dx.doi.org/10.1038/nmeth.2413>

Shannon, C.E. 1949. Communication in the presence of noise. *Proc. IEEE. Inst. Electr. Electron Eng.* 37:10–21.

Sharonov, A., and R.M. Hochstrasser. 2006. Wide-field subdiffraction imaging by accumulated binding of diffusing probes. *Proc. Natl. Acad. Sci. USA.* 103:18911–18916. <http://dx.doi.org/10.1073/pnas.0609643104>

Sheppard, C. 1988. Super-resolution in confocal imaging. *Optik (Stuttg.).* 80:53–54.

Sheppard, C.J.R., S.B. Mehta, and R. Heintzmann. 2013. Superresolution by image scanning microscopy using pixel reassignment. *Opt. Lett.* 38:2889–2892. <http://dx.doi.org/10.1364/OL.38.002889>

Shroff, H., C.G. Galbraith, J.A. Galbraith, H. White, J. Gillette, S. Olenych, M.W. Davidson, and E. Betzig. 2007. Dual-color superresolution imaging of genetically expressed probes within individual adhesion complexes. *Proc. Natl. Acad. Sci. USA.* 104:20308–20313. (published erratum appears in *Proc. Natl. Acad. Sci. USA.* 2008. 105:15220) <http://dx.doi.org/10.1073/pnas.0710517105>

Shroff, H., C.G. Galbraith, J.A. Galbraith, and E. Betzig. 2008. Live-cell photoactivated localization microscopy of nanoscale adhesion dynamics. *Nat. Methods.* 5:417–423. <http://dx.doi.org/10.1038/nmeth.1202>

Sidenstein, S.C., E. D'Este, M.J. Böhm, J.G. Danzl, V.N. Belov, and S.W. Hell. 2016. Multicolour multilevel STED nanoscopy of actin/spectrin organization at synapses. *Sci. Rep.* 6:26725. <http://dx.doi.org/10.1038/srep26725>

Sinkó, J., R. Kákonyi, E. Rees, D. Metcalf, A.E. Knight, C.F. Kaminski, G. Szabó, and M. Erdélyi. 2014. TestSTORM: Simulator for optimizing sample labeling and image acquisition in localization based super-resolution microscopy. *Biomed. Opt. Express.* 5:778–787. <http://dx.doi.org/10.1364/BOE.5.000778>

Sivaguru, M., M.A. Urban, G. Fried, C.J. Wesseln, L. Mander, and S.W. Punyasena. 2016. Comparative performance of airyscan and structured illumination superresolution microscopy in the study of the surface texture and 3D shape of pollen. *Microsc. Res. Tech.* <http://dx.doi.org/10.1002/jemt.22732>

Small, A., and S. Stahlheber. 2014. Fluorophore localization algorithms for super-resolution microscopy. *Nat. Methods.* 11:267–279. <http://dx.doi.org/10.1038/nmeth.2844>

Stelzer, E. 1998. Contrast, resolution, pixelation, dynamic range and signal-to-noise ratio: fundamental limits to resolution in fluorescence light microscopy. *J. Microsc.* 189:15–24. <http://dx.doi.org/10.1046/j.1365-2818.1998.00290.x>

Szymborska, A., A. de Marco, N. Daigle, V.C. Cordes, J.A.G. Briggs, and J. Ellenberg. 2013. Nuclear pore scaffold structure analyzed by super-resolution microscopy and particle averaging. *Science.* 341:655–658. <http://dx.doi.org/10.1126/science.1240672>

Takasaki, K.T., J.B. Ding, and B.L. Sabatini. 2013. Live-cell superresolution imaging by pulsed STED two-photon excitation microscopy. *Biophys. J.* 104:770–777. <http://dx.doi.org/10.1016/j.bpj.2012.12.053>

Tam, J., G.A. Cordier, J.S. Borbely, A. Sandoval Álvarez, and M. Lakadamyali. 2014. Cross-talk-free multi-color STORM imaging using a single fluorophore. *PLoS One.* 9. (published erratum appears in *PLoS One.* 2014. 9) <http://dx.doi.org/10.1371/journal.pone.0101772>

Tang, Y., J. Hendriks, T. Gensch, L. Dai, and J. Li. 2016. Automatic Bayesian single molecule identification for localization microscopy. *Sci. Rep.* 6:33521. <http://dx.doi.org/10.1038/srep33521>

Thompson, R.E., D.R. Larson, and W.W. Webb. 2002. Precise nanometer localization analysis for individual fluorescent probes. *Biophys. J.* 82:2775–2783. [http://dx.doi.org/10.1016/S0006-3495\(02\)75618-X](http://dx.doi.org/10.1016/S0006-3495(02)75618-X)

Tokunaga, M., N. Imamoto, and K. Sakata-Sogawa. 2008. Highly inclined thin illumination enables clear single-molecule imaging in cells. *Nat. Methods.* 5:159–161. <http://dx.doi.org/10.1038/nmeth1171>

Toomre, D., and J. Bewersdorf. 2010. A new wave of cellular imaging. *Annu. Rev. Cell Dev. Biol.* 26:285–314. <http://dx.doi.org/10.1146/annurev-cellbio-100109-104048>

van de Linde, S., U. Endesfelder, A. Mukherjee, M. Schüttelpehl, G. Wiebusch, S. Wolter, M. Heilemann, and M. Sauer. 2009. Multicolor photoswitching microscopy for subdiffraction-resolution fluorescence imaging. *Photochem. Photobiol. Sci.* 8:465–469. <http://dx.doi.org/10.1039/b822533h>

van de Linde, S., S. Wolter, M. Heilemann, and M. Sauer. 2010. The effect of photoswitching kinetics and labeling densities on super-resolution fluorescence imaging. *J. Biotechnol.* 149:260–266. <http://dx.doi.org/10.1016/j.jbiotec.2010.02.010>

Vaughan, J.C., S. Jia, and X. Zhuang. 2012. Ultrabright photoactivatable fluorophores created by reductive caging. *Nat. Methods.* 9:1181–1184. <http://dx.doi.org/10.1038/nmeth.2214>

Venkataramani, V., F. Herrmannsdörfer, M. Heilemann, and T. Kuner. 2016. SuReSim: simulating localization microscopy experiments from ground truth models. *Nat. Methods.* 13:319–321. <http://dx.doi.org/10.1038/nmeth.3775>

Verdaasdonk, J.S., A.D. Stephens, J. Haase, and K. Bloom. 2014. Bending the rules: widefield microscopy and the Abbe limit of resolution. *J. Cell. Physiol.* 229:132–138. <http://dx.doi.org/10.1002/jcp.24439>

Vogel, G. 2015. Sleuthing sheds light on STAP cell fiasco. *Science.* 349:1430–1431. <http://dx.doi.org/10.1126/science.349.6255.1430>

von Diezmann, A., M.Y. Lee, M.D. Lew, and W.E. Moerner. 2015. Correcting field-dependent aberrations with nanoscale accuracy in three-dimensional single-molecule localization microscopy. *Optica.* 2:985–993. <http://dx.doi.org/10.1364/OPTICA.2.000985>

Wäldchen, S., J. Lehmann, T. Klein, S. van de Linde, and M. Sauer. 2015. Light-induced cell damage in live-cell super-resolution microscopy. *Sci. Rep.* 5:15348. <http://dx.doi.org/10.1038/srep15348>

Wang, Y., J. Schnitzbauer, Z. Hu, X. Li, Y. Cheng, Z.-L. Huang, and B. Huang. 2014. Localization events-based sample drift correction for localization microscopy with redundant cross-correlation algorithm. *Opt. Express.* 22:15982–15991. <http://dx.doi.org/10.1364/OE.22.015982>

Waters, J.C. 2007. Live-cell fluorescence imaging. *Methods Cell Biol.* 81:115–140. [http://dx.doi.org/10.1016/S0091-679X\(06\)81007-1](http://dx.doi.org/10.1016/S0091-679X(06)81007-1)

Waters, J.C. 2009. Accuracy and precision in quantitative fluorescence microscopy. *J. Cell Biol.* 185:1135–1148. <http://dx.doi.org/10.1083/jcb.2.00903097>

Weber, K., P.C. Rathke, and M. Osborn. 1978. Cytoplasmic microtubular images in glutaraldehyde-fixed tissue culture cells by electron microscopy and by immunofluorescence microscopy. *Proc. Natl. Acad. Sci. USA.* 75:1820–1824. <http://dx.doi.org/10.1073/pnas.75.4.1820>

Weber, M., M. Mickoleit, and J. Huisken. 2014. Light sheet microscopy. *Methods Cell Biol.* 123:193–215. <http://dx.doi.org/10.1016/B978-0-12-420138-5.00011-2>

Whelan, D.R., and T.D.M. Bell. 2015. Image artifacts in single molecule localization microscopy: why optimization of sample preparation protocols matters. *Sci. Rep.* 5:7924. <http://dx.doi.org/10.1038/srep07924>

Wolter, S., A. Löschberger, T. Holm, S. Aufmkolk, M.-C. Dabauvalle, S. van de Linde, and M. Sauer. 2012. rapidSTORM: accurate, fast open-source software for localization microscopy. *Nat. Methods.* 9:1040–1041. <http://dx.doi.org/10.1038/nmeth.2224>

Wu, J.-Q., and T.D. Pollard. 2005. Counting cytokinesis proteins globally and locally in fission yeast. *Science.* 310:310–314. <http://dx.doi.org/10.1126/science.1113230>

Wurm, C.A., K. Kolmakov, F. Göttfert, H. Ta, M. Bossi, H. Schill, S. Berning, S. Jakobs, G. Donnert, V.N. Belov, and S.W. Hell. 2012. Novel red fluorophores with superior performance in STED microscopy. *Opt. Nanoscopy.* 1:7. <http://dx.doi.org/10.1186/2192-2853-1-7>

Yildiz, A., J.N. Forkey, S.A. McKinney, T. Ha, Y.E. Goldman, and P.R. Selvin. 2003. Myosin V walks hand-over-hand: single fluorophore imaging with 1.5-nm localization. *Science.* 300:2061–2065. <http://dx.doi.org/10.1126/science.1084398>

York, A.G., P. Chandris, D.D. Nogare, J. Head, P. Wawrzusin, R.S. Fischer, A. Chitnis, and H. Shroff. 2013. Instant super-resolution imaging in live cells and embryos via analog image processing. *Nat. Methods.* 10:1122–1126. <http://dx.doi.org/10.1038/nmeth.2687>